



ESPE
UNIVERSIDAD DE LAS FUERZAS ARMADAS
INNOVACIÓN PARA LA EXCELENCIA

**Comparison of control strategies for monitoring the maximum power point
tracking of a photovoltaic plant**

Intriago Laverde, Sofía Liseña y Robayo Arcos, Paola Fernanda

Departamento de Eléctrica y Electrónica

Carrera de Ingeniería Electrónica e Instrumentación

Artículo académico, previo a la obtención del título de Ingeniera en Electrónica e

Instrumentación

Ing. Llanos Proaño, Jacqueline del Rosario MSc. PhD

15 de agosto del 2022

Latacunga



ETCM-FINAL_Control_PanelesSolar.pdf

Scanned on: 13:20 August 15, 2022 UTC



Overall Similarity Score



Results Found



Total Words in Text

Identical Words	74
Words with Minor Changes	1
Paraphrased Words	0
Omitted Words	15



Firmado electrónicamente por:
JACQUELINE DEL
ROSARIO LLANOS
PROANO



Departamento de Eléctrica y Electrónica

Carrera de Ingeniería Electrónica e Instrumentación

Certificación

Certifico que el artículo académico: "**Comparison of control strategies for monitoring the maximum power point tracking of a photovoltaic plant**" fue realizado por las señoritas **Intriago Laverde, Sofía Liseña y Robayo Arcos, Paola Fernanda**, el mismo que cumple con los requisitos legales, teóricos, científicos, técnicos y metodológicos establecidos por la Universidad de las Fuerzas Armadas ESPE, además fue revisado y analizado en su totalidad por la herramienta de prevención y/o verificación de similitud de contenidos; razón por la cual me permito acreditar y autorizar para que se lo sustente públicamente.

Latacunga, 15 de agosto del 2022

Firma:

Llanos Proaño, Jacqueline del Rosario

Directora

C. C.: 0502527039



Departamento de Eléctrica y Electrónica

Carrera de Ingeniería Electrónica e Instrumentación

Responsabilidad de Autoría

Nosotras, **Intriago Laverde, Sofía Liseña** con cédula de ciudadanía N° 1724385834 y **Robayo Arcos, Paola Fernanda**, con cédula de ciudadanía N° 1803991544 declaro que el contenido, ideas y criterios del artículo académico: **Comparison of control strategies for monitoring the maximum power point tracking of a photovoltaic plant** es de nuestra autoría y responsabilidad, cumpliendo con los requisitos legales, teóricos, científicos, técnicos, y metodológicos establecidos por la Universidad de las Fuerzas Armadas ESPE, respetando los derechos intelectuales de terceros y referenciando las citas bibliográficas.

Latacunga, 15 de agosto del 2022

Firma:

Intriago Laverde Sofía Liseña
C.C.: 1724385834

Robayo Arcos Paola Fernanda
C.C: 1803991544



Departamento de Eléctrica y Electrónica

Carrera de Ingeniería Electrónica e Instrumentación

Autorización de Publicación

Nosotras, **Intriago Laverde, Sofía Liseña Liseña** con cédula de ciudadanía N° 1724385834 y **Robayo Arcos, Paola Fernanda**, con cédula de ciudadanía N° 1803991544 autoras del artículo académico: **Comparison of control strategies for monitoring the maximum power point tracking of a photovoltaic plant** autorizamos a la Universidad de las Fuerzas Armadas ESPE publicar en el Repositorio Institucional: el registro bibliográfico, el resumen y la dirección web indexada en la revista.

Latacunga, 15 de agosto del 2022

Firma

Intriago Laverde Sofía Liseña
C.C.: 1724385834

Robayo Arcos Paola Fernanda
C.C.: 1803991544



Departamento de Eléctrica y Electrónica

Carrera de Ingeniería Electrónica e Instrumentación

Carta de Compromiso

Yo **Llanos Proaño, Jacqueline del Rosario**, con cédula de ciudadanía N° 0502527039 en mi calidad de Director del artículo académico: **Comparison of control strategies for monitoring the maximum power point tracking of a photovoltaic plant**, de las autoras: **Intriago Laverde, Sofía Liseña Liseña y Robayo Arcos, Paola Fernanda**, me comprometo a entregar a la Dirección de Carrera, la dirección web indexada en la revista del artículo en mención, una vez que el mismo sea publicado, con la finalidad de que finalmente sea incluido dentro de los metadatos del Repositorio Institucional.

Firma

Llanos Proaño, Jacqueline del Rosario

Directora

C. C.: 0502527039

Comparison of control strategies for monitoring the maximum power point tracking of a photovoltaic plant

Sofia Intriago
Dept. Eléctric and Electronic
Universidad de las Fuerzas Armadas
ESPE
Latacunga, Ecuador
slintriago2@espe.edu.ec

Franklin Silva
Universidad de las Fuerzas Armadas
ESPE
Latacunga, Ecuador
fmsilva@espe.edu.ec

Paola Robayo
Dept. Eléctric and Electronic
Universidad de las Fuerzas Armadas
ESPE
Latacunga, Ecuador
pfrobayo@espe.edu.ec

Juan Gómez
Departamento de Ingeniería
Universidad Andrés Bello
Santiago, Chile
juansebastiangomezq@gmail.com

Jacqueline Llanos
Dept. Eléctric and Electronic
Universidad de las Fuerzas Armadas
ESPE
Latacunga, Ecuador
jlllanos1@espe.edu.ec

Abstract— The solar resource is an unlimited source to generate energy, however, specific features such as irradiance and temperature, as well as the panel construction affect the system performance, thus, also changing the maximum power deliverable for the photovoltaic system. In this sense, a controller designed for Maximum Power Point Tracking (MPPT) is required to seek the operation voltage (V_{mpp}) and current (I_{mpp}), therefore, increasing the system efficiency. In this paper traditional MPPT control techniques, Perturb and observe (P&O) and incremental conductance (INC), are compared to advanced control techniques Fuzzy Logic Controller (FCL) and Finite Control Set - Model Predict Control (FCS-MPC). The simulations, implemented in Matlab/Simulink, take the two-step ahead FCS MPC as the best controller for a photovoltaic system.

Keywords— DC/DC boost converter, MPPT, P&O, INC, FLC, FCS MPC.

I. INTRODUCTION

In recent decades, the efficient use of alternative energy compared to conventional power has increased unquestionably [1]. The fossil resource decrease, added to a highly polluting process, can be contrasted unstopable interest in clean energies applications, contribute to reducing CO₂ emissions is essential [2],[3]; according statistics shown by the International Renewable Energy Agency (IRENA) [4].

The regulations help to regulate the use of this type energy established around the world, simultaneously promoting self-consumption and the installation of modern solar applications both in Europa [5] and Latin America [6],[7],[8]; thus, through the creation of new conformity assessment systems for renewable energies, humanity hopes overcome the zero net carbon emissions plan by the year 2050 [9],[10].

The sun is a powerful renewable energy resources which is constantly changing according to weather (irradiance, temperature, clouds, etc.). Although these changes, studies have been shown that using the Maximum Power Point Tracking (MPPT) technique, power extraction is maximized [11],[12]. Perturb and observe (P&O), and Incremental Conductance (INC) algorithms have been widely reported in literature. Both techniques disturb operation voltages and/or

currents, then measure its impact in order to identify the MPP [13],[14]. Their main advantage is the direct computation of the duty cycle used for switching semiconductors on DC-DC power converters. A detailed description of these algorithms will be presented in section III.

Advanced control strategies such as Fuzzy Logic Controller (FLC), Artificial Neural Networks (ANN), and Model based Predictive Control (MPC) have been also reported for MPPT applications, FLC present a robustness feature when information about the system inputs is imprecise, non-linearities are considered or operator expertise will be integrated [16]. In [17], [18] MPPTs based on artificial neural networks (ANN) are report. Those schemes use at least three layers to obtain the duty cycle required to control the output voltage at the MPP. Another implementation of an ANN composed of four layers, reported in [19] is to estimate the variable step-size VSS for the perturbation in the INC MPPT algorithm with an adaptive scale factor. In this case, the optimal scaling factor (OSF) is entered in MPPT to obtain a fast and accurate tracking response. Because of advances in microelectronics, processing capacity is increasing, allowing the integration of MPC in real-time control tasks, such as power electronics. Finite Control Set MPC (FCS-MPC) and Continuous Control Set MPC (CCS-MPC), are the main two trends in MPC applications. FCS MPC applies intuitive concepts to non-linear systems such as power converters, by using multiple control objectives with multiple inputs, a significant advantage of this scheme is the finite number of solution states, providing more deployability for real-time applications [20],[21],[22]. In contrast, because of the continuous solution space of CCS-MPC, a modulation scheme such as Pulse Width Modulation (PWM) is required to compute the duty cycle of semiconductors switches. An application of this technique is shown in [23] which uses the MPPT INC algorithm with a two-step prediction with two control objectives in panel photovoltaic (PV) voltage and current (V_{pv} , I_{pv}).

This research focuses on comparing the PV system efficiency, as well as the maximum power generated among different control techniques applied to the DC/DC boost converter.

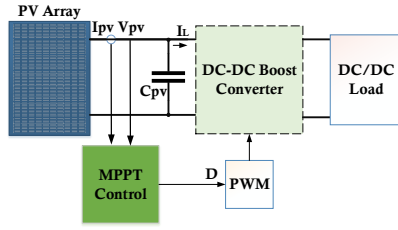


Fig. 1 Controlled photovoltaic system diagram

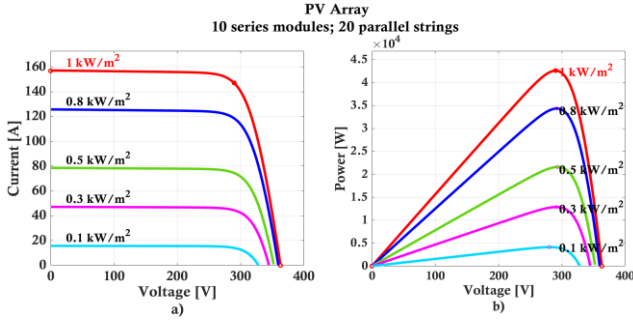


Fig. 2 a) Current VS Voltage performance curve, b) Power VS Voltage performance curve of the solar panel array

The main contribution of this work is the evaluation by simulation, the comparison, and identification of the advantages and disadvantages of the control algorithms applied by MPPT, both for traditional control techniques such as Perturb and Observe (P&O) [13], Incremental Conductance (INC) [15],[16], as well as for advanced control techniques such as Fuzzy Logic [24],[25], and Model-Based Predictive Control, it was decided to use the two-step horizon FSC MPC technique in conjunction with the current P&O algorithm [23],[26]; in the MATLAB/Simulink program, determine which of these techniques is the most suitable for MPPT to have an optimal algorithm.

II. DESCRIPTION OF THE PHOTOVOLTAIC SYSTEM

A typical photovoltaic system, as show in Fig. 1 is composed of a PV array, an input capacitor (C_{pv}) a DC-DC boost converter, an MPPT control block, and a local DC load. The signals measurements of the photovoltaic system (V_{pv} , I_{pv}) and the coil current (I_L), at the PV side, allow to compute the duty cycle signal (D), which allows the pulse width modulation (PWM) to transfer the switching signal to the DC/DC boost converter.

A. Description-operation of PV

The sizing of the PV array depends on the solar resource available and the power capacity constraints of DC-DC converter. In some case series/parallel arrangements are required to increase output voltage and current depends on the available solar resource and the load to be supplied [27] Considering their characteristic curves, PV arrays are usually modeled as current sources. Fig. 2a) shows the characteristic curve I_{pv} vs. V_{pv} , and Fig. 2b) shows the characteristic curve of Power (P_{pv} vs. V_{pv}) at different values of irradiance, being evident how the MPP varies.

Internal and external factors influence the PV array behavior, such as the shape and material of manufacture, facilities, humidity, environment weather, excessive dust,

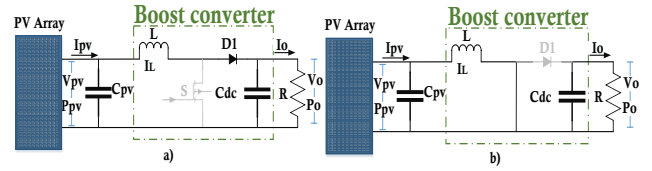


Fig. 3 DC/DC Boost converter circuit a) On-State mode b) Off-State mode

and shadows. Depending on the facilities wide, shadows over the PV array can cause local maximum power points, making it challenging to achieve the MPP, affecting the photovoltaic system efficiency and performance [16].

A. D/D Boost converter

The boost converter shown in Fig. 3 operates according to the transistor (S) state. When transistor S is open, Fig. 3a), the diode (D1) conducts through the capacitance (C_{dc}) until it is fully charged and through the local resistive load (R). On the other hand, when S is closed Fig. 3b) the source charges the inductor (L), meanwhile R is fed from C_{dc} .

Equations (1)- (9) define the continuous operation mode for the regular operation of the transistor S [28]. Having a variable input voltage of the photovoltaic cell (V_{pv}), the change in the value of D according to (1) is required to following the MPP by changing the output voltage of the DC/DC boost converter (V_o). Assuming a circuit without losses, that is, the input power is equal to the output, (2) is obtained, where I_{pv} is the input current, and I_o is the output current. Replacing as current function, (3) is obtained.

$$\frac{V_o}{V_{pv}} = \frac{1}{1-D} \quad (1)$$

$$V_{pv} \cdot I_L = V_o \cdot I_o \quad (2)$$

$$\frac{I_o}{I_L} = (1-D) \quad (3)$$

Therefore, to find the inductor L and the capacitor C_{dc} , in (4) and (5), R of the load is required, T represents the work period, and ΔV_o is the variation of the output voltage.

$$L > R \cdot D \cdot (1-D)^2 \cdot \frac{T}{2} \quad (4)$$

$$C_{dc} = \frac{P_o \cdot D \cdot T}{V_o \cdot \Delta V_o} \quad (5)$$

The differential equations in (6) and (9) represent the system; for previously found data of L and C_{dc} , with the variability of the current and voltage present [26]. In (6) and (7) are when S is open, as shown in Fig. 3a)

$$\frac{dI_L}{dt} = -\frac{1}{L} \cdot V_o + \frac{1}{L} \cdot V_{pv} \quad (6)$$

$$\frac{dV_o}{dt} = -\frac{1}{C_{dc}} I_L - \frac{1}{R \cdot C_{dc}} \cdot V_o \quad (7)$$

In (8) and (9) represent the system when S is closed, as in Fig. 3b)

$$\frac{dI_L}{dt} = \frac{1}{L} \cdot V_{pv} \quad (8)$$

$$\frac{dV_o}{dt} = -\frac{1}{R \cdot Cdc} \cdot V_o \quad (9)$$

III. DESIGN OF MPPT CONTROL STRATEGIES FOR THE DC/DC BOOST CONVERTER

In this section, traditional MPPT control techniques: disturbs and observe, and incremental conductance are described. In addition, two advanced control strategies, the first based on fuzzy logic and the second based on model-based predictive control are also presented.

A. Control Algorithm Perturb and Observe

Perturb and observe (P&O) algorithm has been reported to achieve the MPPT, by disturbing the system voltage in $k+1$, since voltage and currents captured in instant k . Power computation is compared to the power of the photovoltaic output at the previous cycle ($k-1$) [13]. The main drawback is that when it reaches the Maximum Power Point (MPP), it oscillates, which causes losses of photovoltaic energy. The large size of the disturbance causes the oscillations since if it is small, it will slow down the MPPT. The reference voltage (V_{pv}^*) at the instant k determines the direction of the next disturbance [14]. Fig. 4 shows the flow diagram of the P&O algorithm, where the increase or decrease of PV power and voltage modifies V_{pv}^* is utilized for the PI control loop for the generation of D .

B. Control algorithm Incremental Conductance

In [14], the incremental conductance technique (INC) is reported. In this case, voltage and current measurements (V_{pv} , I_{pv}) are captured at k , then are compared to the measurements of the previous cycle $k-1$ in order to compute the incremental conductance. Fig. 5 shows the flow chart of this algorithm. When the voltage and current coincide at zero, the MPP is achieved, therefore no changes in D are required. Otherwise, the value of D is computed as a function of the interpretation of the conductance ($\Delta I_L/\Delta V_{pv}$) and current variation (ΔI_L). This algorithm identifies when the MPP has been reached, so fast action gets over than P&O, though increases in complexity compared to the previous algorithm [15].

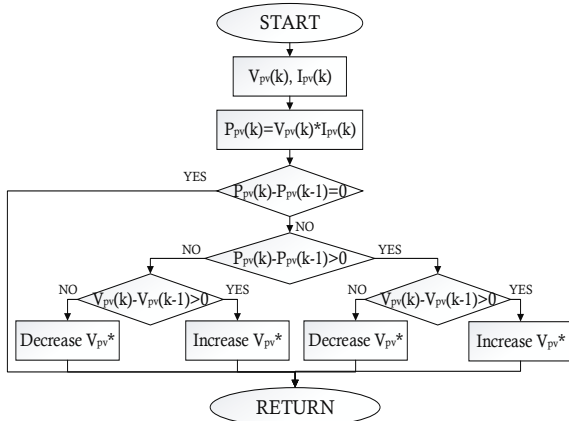


Fig. 4 Perturb-and-observe algorithm flowchart

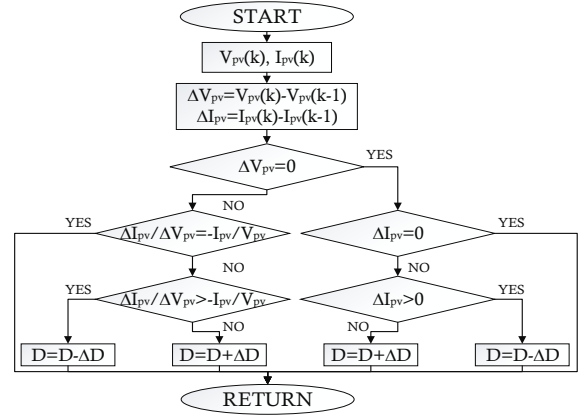


Fig. 5 Incremental conductance algorithm flowchart

C. Controller-based on Fuzzy Logic

The application of this control algorithm is simplified since Mamdanis inference is used, thus a mathematical model is not required. The controller consists of four essential parts: fuzzification, the rule base, the inference machine, and defuzzification. Although computational burden of this type of controllers increase according to P&O and INC, the integration of operator expertise, as well as to avoiding a precise non-linear model are clear advantages [16]. Fig. 6 shows the fuzzy logic (FL) based control design, where the selected inputs $E(k)$ and $CE(k)$, obtained in (10) and (11), are represented respectively [29].

$$E(k) = \frac{P_{pv}(k) - P_{pv}(k-1)}{I_{pv}(k) - I_{pv}(k-1)} \quad (10)$$

$$CE(k) = E(k) - E(k-1) \quad (11)$$

Where $E(k)$ is the voltage variation and $CE(k)$ is E variation. A well-known fuzzy inference method is Mamdani's method with the maximum-minimum operation fuzzy combination law. The defuzzification stage uses the centroid method. The five fuzzy sets represented in the trapezoidal membership functions are Negative Big (NB) and Positive Big (PB) for the two inputs. Negative Big (NB) and Positive Big (PB) for the two inputs. In contrast, the triangular functions are Negative Small (NS), Zero (ZE), and Positive Small (PS) fuzzy sets. (See Fig. 7 a) and Fig. 7 b)). The output variable uses five fuzzy sets with the same linguistic variables as the inputs and with fuzzy sets of central triangular functions and trapezoidal functions at the ends (See Fig. 7 c)) [16]. Combining the fuzzy sets of the inputs results in twenty-five rules, shown in TABLE I [24].

TABLE I CONTROLLER RULES BASED ON FUZZY LOGIC

CE/E	NB	NS	ZE	PS	PB
NB	NB	NB	NB	NS	ZE
NS	NB	NB	NS	ZE	PS
ZE	NB	NS	ZE	PS	PB
PS	NS	ZE	PS	PB	PB
PB	ZE	PS	PB	PB	PB

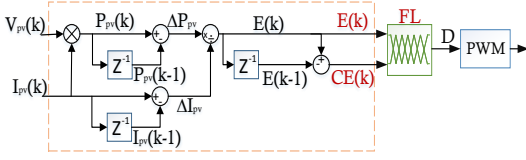


Fig. 6 Diagram of the fuzzy logic-based control algorithm for MPPT

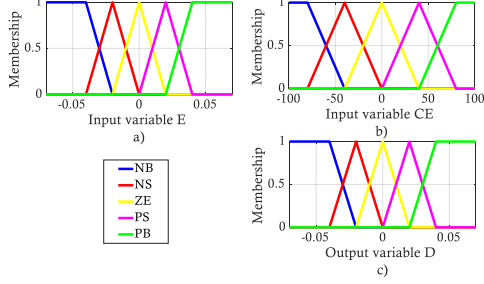


Fig. 7 Fuzzy set of the variables, a) Fuzzy set of the input E, b) Fuzzy set of the input CE, c) Fuzzy sets of the output

D. FCS-MPC for MPPT

The FCS-MPC scheme computes and compare the all possible output states based on a discrete time model of power converter, choosing the output which represents the lower cost according to a cost function related to the control objectives [20]. As shown in Fig. 8 the proposed scheme uses a modified P&O algorithm (See Fig. 9) to compute the current reference (I_L^*) used by the MPC cost function J for optimizing output voltage and current as well as the compensation term E . The cost function requires the prediction model of I_L and V_o at two steps of the prediction horizon [26].

The aforementioned modified P&O algorithm is based on [21], and disturbs output current, instead of voltage, as the one presented in section III A. Two current increments are stated (I_{d1} , I_{d2}). The modification that is in the two increment values in question (I_{d1} , I_{d2}), that as consequently (I_d) will change depending on the ΔI_{pv} and (I_s) of ΔI_{PV} (k) in one iteration. When irradiance varies a little, (P_s) take a predefined value of ΔP_{pv} (k) in one iteration; the significant difference in irradiance will detect sudden changes based on the variation of power (ΔP_{pv}), where P_s influences the flow of the algorithm, besides optimal scale factor (K_{opT}) with range [0.8; 0.92], see Fig. 9. The cost function requires the prediction model of I_L and V_o at two steps of the prediction horizon.

Because of FCS-MPC requires a discrete time model, equations (6) to (9) are transformed by using Euler discretization (12), where T_s is the sampling period [23], [26].

$$\frac{dz(k)}{dt} \approx \frac{z(k+1) - z(k)}{T_s} \quad (12)$$

Now to be able to predict in two or more steps, (13) and (14) are used, which indicate n-sampling of instants needed in the future for optimal control, where $(1-s)$ indicates the possible switching states [0 1], without causing alteration in the calculation of I_L and V_o [23].

$$I_{L,s} = I_L(k+n-1) - (1-s) \frac{T_s}{L} \cdot V_o(k+n-1) + \frac{T_s}{L} \cdot V_{pv}(k+n-1) \quad (13)$$

$$V_{O,s} = (1-s) \frac{T_s}{C_{dc}} \cdot I_L(k+n-1) + \left(1 - \frac{T_s}{R \cdot C_{dc}}\right) \cdot V_o(k+n-1) \quad (14)$$

Considering two steps ahead, the state space representation is presented in (15). $I_L(k+1)$ and $V_o(k+1)$ are calculated with $n=1$ in (19) and for $V_{pv}(k+1)$, it is calculated by using LaGrange interpolation method of (16) with $a=1$ specified in [23], Then (17) is stated.

$$\begin{bmatrix} I_L(k+2) \\ V_o(k+2) \end{bmatrix} = \begin{bmatrix} 1 & -(1-s) \frac{T_s}{L} \\ (1-s) \frac{T_s}{C_{dc}} & 1 - \frac{T_s}{R \cdot C_{dc}} \end{bmatrix} \begin{bmatrix} I_L(k+1) \\ V_o(k+1) \end{bmatrix} + \begin{bmatrix} \frac{T_s}{L} \\ 0 \end{bmatrix} \cdot V_{pv}(k+1) \quad (15)$$

The cost function (18) controls I_L and V_o , with a regulation factor $E_{s=n}$, where α and β are weighting factors in a range of [0-1]. $E_{s=n}$ is the prediction error of the value of $V_{pv}(k+1) - V_{pv}(k)$.

$$V_{pv}(k+1) = \sum_{l=0}^a (-1)^{a-1} \binom{a+1}{l} \cdot V_{pv}(k+1-a) \quad (16)$$

$$V_{pv}(k+1) = 2V_{pv}(k) - V_{pv}(k-1) \quad (17)$$

$$J_{s=n}^{n=0,1 \text{ \& } m=0,1} = \alpha \cdot |I_{L,s=m}(k+2) - I_L^*| + \beta \cdot |V_{o,s=m}(k+2) - V_o^*| + E_{s=n} \quad (18)$$

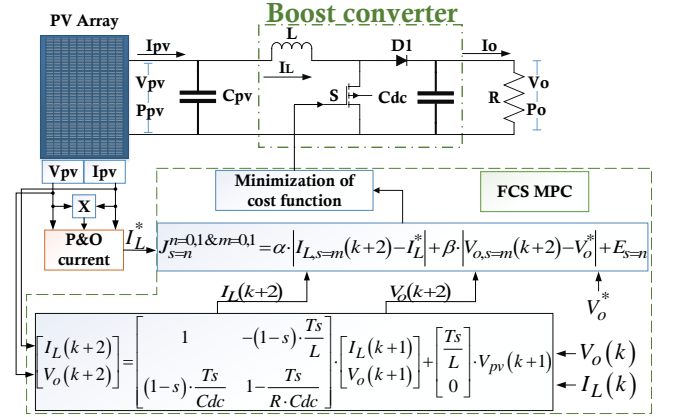


Fig. 8 FCS-MPC Control Algorithm Diagram

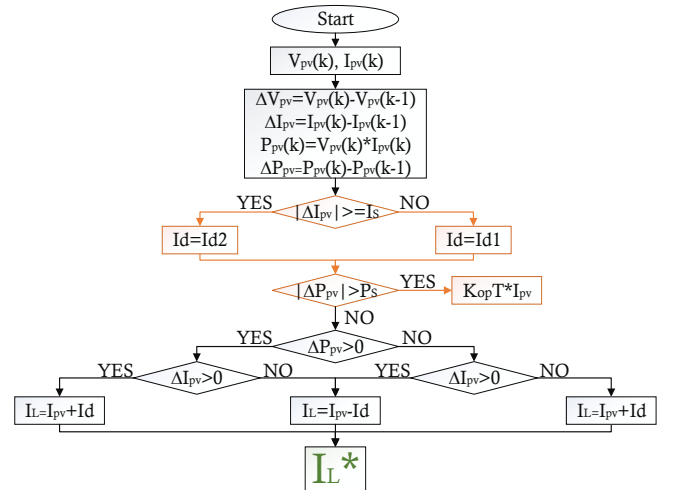


Fig. 9 Algorithm of perturb and observes of current

IV. RESULTS

TABLE II PV MODULES SET PARAMETE

PV Model	1Soltech STH-215-P
Open circuit voltage Voc (V)	36,3
Short circuit current Isc (A)	7,84
Temperature coefficient of Voc (%/deg. C)	-0,36099
Temperature coefficient of Isc (%/deg. C)	0,102
Pmpp (W)	213,15
Vmpp(V)	29
Impp(A)	7,35
Efficiency (η)	13,7%

The configuration of the simulated PV array is shown in TABLE II with twenty solar panels in parallel that increase the system current from 7.84 A to 156 A and ten solar panels in series, which increase the voltage from 36.3 V to 363 V. In TABLE III shows the parameters of the DC/DC boost converter.

TABLE III DC/DC BOOST CONVERTER DESIGN PARAMETERS

Description	Symbol	Value	Unit
Inductor	L	4,56	[mH]
Input capacitor	Cpv	519	[μ F]
Output capacitor	Cdc	519	[μ F]
Load resistance	R	30	[Ω]
Sampling time	Ts	200	[μ s]
Input Voltage	Vpv	250	[V]
Power	Ppv	42,630	[kW]
Frecuency switching	fs	5	[kHz]

The proposed techniques successfully calculate the ideal Ppv shown in Fig. 2, fulfilling the objective of improving the efficiency of the photovoltaic system. For Case a two-step irradiance profile (Fig. 12a)) and the powers generated with the different control strategies evaluated are obtained as shown in Fig. 13; where ideally, the powers at these operating points correspond to 42, 5 [kW], and 34.33 [kW]. The FCS-MPC algorithm in steady state is closer to the ideal value calculated with an approximation of 99.68%, while the FLC control the deviations are more extensive. The approximation is 79.30%, and the rest algorithms also

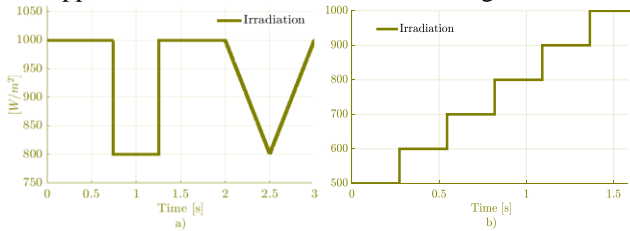


Fig. 10 Irradiance profiles

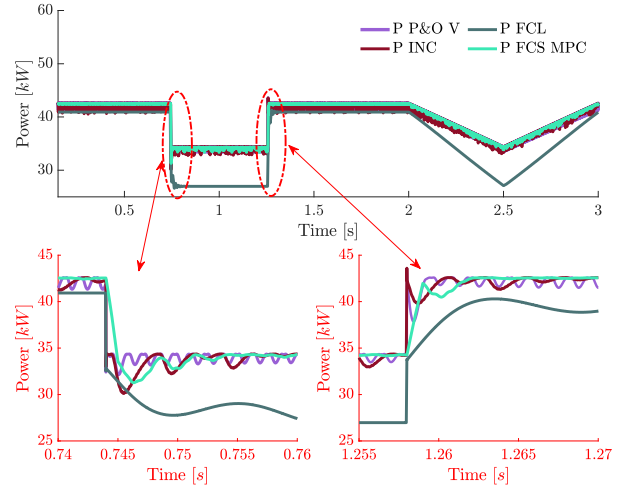


Fig. 11 Results of Case a

approach the ideal value; however, they present oscillations. The transitory state is also analyzed in the boxes of maximized Fig. 13, showing a better performance with the FCS MPC due to less overshoot and undershoot. The powers with P&O and INC show oscillations.

The different types of irradiance tests for case b are prominent (See Fig. 12), in which the profile from 0 to 3[s] is of the ascending step type from 500 to 1000[W/m²]. Applying the different control algorithms in simulation, with an objective of 42.5 [kW] and 34.33 [kW] of ideal power; Fig. 14 shows the FLC controller contains an approximation of 73.56%, so its deviation is more significant; while FCS maintains the station state close to the ideal value with an approximation of 99.99%. During the simulation, the oscillations in the output powers of the other controllers are notorious. However, they are pretty similar to the ideal value, which shows that FCS MPC shows low overshoot and undershoot, so its performance stands out among the other algorithms.

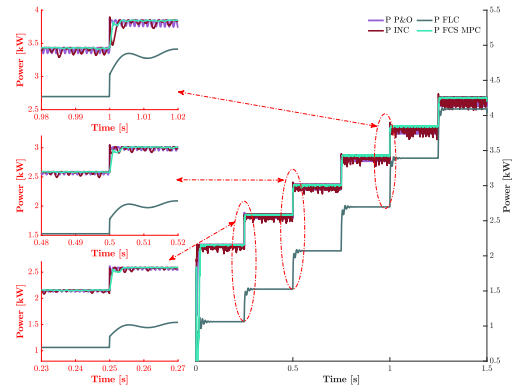


Fig. 12 Results of Case b

V. CONCLUSIONS

In this work, four MPPT-based control algorithms are compared with each other so that the PV array captures the greatest energy. The algorithms evaluated are Perturb and Observe, Incremental Conductance, Fuzzy Logic Control, And Predictive Control Based On Finite Control Set Model in different irradiance scenarios. The FCS MPC control algorithm has shown better performance concerning a degree of similarity to the ideal value of 99.99%, which is

higher than the other controllers. However, this controller presents a higher computational burden than other controllers; it is about 327.82 μ s and 259.31 μ s in both cases of the irradiance profile tested, P&O has 0.81 μ s, and the computational burden of INC is 0.46 μ s. Traditional algorithms like P&O have a degree of similarity to the ideal of 99,85%, and INC shows a degree of similarity to the ideal of 99,89%. FLC controller offers a lower efficiency than the different algorithms; however, it improves the photovoltaic system's stability and its time computational is not far from conventional algorithms.

REFERENCES

- [1] A. M. Omer, Green energies and the environment, *Renewable and Sustainable Energy Reviews*, vol. 12, no. 7, pp. 1789–1821, 2008.
- [2] P. Taylor, T. Abbasi, and S. A. Abbasi, Is the Use of Renewable Energy Sources an Answer to the Problems of Global Warming and Pollution? *Crit. Rev. Environ. Sci. Technol.*, no. July 2013, pp. 37–41, 2011, doi: 10.1080/10643389.2010.498754.
- [3] H. Abu-Rub, M. Malinowski, and K. Al-Haddad, *Power Electronics for Renewable Energy Systems, Transportation and Industrial Applications*. 2014.
- [4] IRENA, Annual Report of the Director-General on the Implementation of the Work Programme and Budget for 2018–2019, no. December 2018, pp. 11–13, 2019.
- [5] D. E.-I. F. European Commission, *Renewable energy in Europe*, no. March, pp. 2020–2022, 2020.
- [6] Ministerio de Energía- República Argentina. <https://www.energia.gob.ar/contenidos/verpagina.php?idpagina=3876> (accessed Mar. 30, 2022).
- [7] CEPAL/GTZ, *Fuentes Renovables de energía en América Latina y el Caribe*, CEPAL, Com. Económica para América Lat. y el Caribe, vol. 53, no. 9, pp. 1689–1699, 2004.
- [8] Asamblea Nacional del Ecuador, *Constitución de la República del Ecuador*, Iusrectusecart, no. 449, pp. 1–219, 2021, [Online]. Available: <https://bde.fin.ec/wp-content/uploads/2021/02/Constitucionultimodif25enero2021.pdf>
- [9] G. Kelly et al., Defining the Value of IECRE Certifications for Providing Confidence in PV System Performance, 2018 IEEE 7th World Conf. Photovolt. Energy Conversion, WCPEC 2018 - A Jt. Conf. 45th IEEE PVSC, 28th PVSEC 34th EU PVSEC, vol. 82, pp. 2422–2425, 2018, doi: 10.1109/PVSC.2018.8547963.
- [10] National Grid ESO, *Future Energy Scenarios Navigation*, no. July, pp. 1–124, 2020, [Online]. Available: <https://www.nationalgrideso.com/future-energy/future-energy-scenarios>.
- [11] D. Cardozo, *Simulación de un Sistema Fotovoltaico Aislado en Matlab / Simulink*, Mundo Fesc, vol. 9, no. 17, p. 7, 2019.
- [12] P. Hurley, *Build Your Own Solar Panel*, 1st ed. USA: Wheelock Mountain Publications, 2006.
- [13] S. K. Sah and K. Thakur, Comparative Simulation Study of Grid Connected Perturb & Observe and Incremental Conductance MPPT Algorithm, pp. 1065–1068, 2020.
- [14] S. A. Mohamed and M. Abd El Sattar, A comparative study of P&O and INC maximum power point tracking techniques for grid-connected PV systems, *SN Appl. Sci.*, vol. 1, no. 2, pp. 1–13, 2019, doi: 10.1007/s42452-018-0134-4.
- [15] M. S. Nkambule, A. N. Hasan, and A. Ali, MPPT under partial shading conditions based on Perturb & Observe and Incremental Conductance, *ELECO 2019 - 11th Int. Conf. Electr. Electron. Eng.*, no. April 2020, pp. 85–90, 2019, doi: 10.23919/ELECO47770.2019.8990426.
- [16] T. Esham and P. L. Chapman, Comparison of photovoltaic array maximum power point tracking techniques, *IEEE Trans. Energy Convers.*, vol. 22, no. 2, pp. 439–449, 2007, doi: 10.1109/TEC.2006.874230.
- [17] F. Sedaghati, A. Nahavandi, M. A. Badamchizadeh, S. Ghaemi, and M. Abedinpour Fallah, PV maximum power-point tracking by using artificial neural network, *Math. Probl. Eng.*, vol. 2012, 2012, doi: 10.1155/2012/506709.
- [18] K. Y. Yap, C. R. Sarimuthu, and J. M. Y. Lim, Artificial Intelligence Based MPPT Techniques for Solar Power System: A review, *J. Mod. Power Syst. Clean Energy*, vol. 8, no. 6, pp. 1043–1059, 2020, doi: 10.35833/MPCE.2020.000159.
- [19] S. Ye, Y. Liu, and C. Liu, Artificial Neural Network Assisted Variable Step Size Incremental Conductance MPPT Method with Adaptive Scaling Factor, 2022.
- [20] J. Rodríguez and P. Cortés, *Predictive Control of Power Converters and Electrical Drives*. 2012.
- [21] J. Rodríguez, J. Pontt, C. Silva, P. Cortés, U. Amman, and S. Rees, Predictive current control of a voltage source inverter, *PESC Rec. - IEEE Annu. Power Electron. Spec. Conf.*, vol. 3, no. 1, pp. 2192–2196, 2004, doi: 10.1109/PESC.2004.1355460.
- [22] F. Blaabjerg, Ed., *Control of power electronic converters and systems*, Volume 3. Academic Press, 2021.
- [23] P. E. Kakosimos and A. G. Kladas, Implementation of photovoltaic array MPPT through fixed step predictive control technique, *Renew. Energy*, vol. 36, no. 9, pp. 2508–2514, 2011, doi: 10.1016/j.renene.2011.02.021.
- [24] M. Fathi and J. A. Parian, “Intelligent MPPT for photovoltaic panels using a novel fuzzy logic and artificial neural networks based on evolutionary algorithms,” *Energy Reports*, vol. 7, pp. 1338–1348, 2021, doi: 10.1016/j.egy.2021.02.051.
- [25] H. Rezk, M. Aly, M. Al-Dhaifallah, and M. Shoyama, Design and Hardware Implementation of New Adaptive Fuzzy Logic-Based MPPT Control Method for Photovoltaic Applications, *IEEE Access*, vol. 7, pp. 106427–106438, 2019, doi: 10.1109/ACCESS.2019.2932694.
- [26] A. Hussain, H. A. Sher, A. F. Murtaza, and K. Al-Haddad, Improved restricted control set model predictive control (iRCS-MPC) based maximum power point tracking of photovoltaic module, *IEEE Access*, vol. 7, pp. 149422–149432, 2019, doi: 10.1109/ACCESS.2019.2946747.
- [27] D. Mayuresh, *Modeling of PV Arrays based on Datasheet* Mayuresh, pp. 1–4, 2016.
- [28] N. Mohan, T. M. Undeland, and W. P. Robbins, *Electrónica de Potencia Convertidores, aplicaciones y diseño*, Tercera. México: McGRAW-HILL/INTERAMERICANA.
- [29] C.-Y. Won, D.-H. Kim, S.-C. Kim, W.-S. Kim, and H.-S. Kim, A New Maximum Power Point Tracker of Photovoltaic Arrays Using Fuzzy Controller, 1994.
- [30] O. Kukrer, Discrete-time current control of voltage-fed three-phase PWM inverters, *IEEE Trans. Power Electron.*, vol. 11, no. 2, pp. 260–269, 1996, doi: 10.1109/63.486174.